metals

MDPI

Article

Leaching Kinetics of Arsenic Sulfide-Containing Materials by Copper Sulfate Solution

Kirill A. Karimov, Denis A. Rogozhnikov, Evgeniy A. Kuzas and Andrei A. Shoppert *

Department of Non-Ferrous Metals Metallurgy, Ural Federal University, 620002 Yekaterinburg, Russia; kirill_karimov07@mail.ru (K.A.K.); darogozhnikov@yandex.ru (D.A.R.); e.kuzas@ya.ru (E.A.K.)
* Correspondence: andreyshop@list.ru; Tel.: +7-922-024-3963

Received: 25 November 2019; Accepted: 16 December 2019; Published: 19 December 2019

Abstract: The overall decrease in the quality of mineral raw materials, combined with the use of arsenic-containing ores, results in large amounts of various intermediate products containing this highly toxic element. The use of hydrometallurgical technologies for these materials is complicated by the formation of multicomponent solutions and the difficulty of separating copper from arsenic. Previously, for the selective separation of As from copper–arsenic intermediates a leaching method in the presence of Cu(II) ions was proposed. This paper describes the investigation of the kinetics of arsenic sulfide-containing materials leaching by copper sulfate solution. The cakes after leaching of arsenic trisulfide with a solution of copper sulfate were described using methods such as X-ray diffraction spectrometry (XRD), X-ray fluorescence spectrometry (XRF), scanning electron microscopy (SEM) and energy-dispersive X-ray spectroscopy analysis (EDS). The effect of temperature (70–90 °C), the initial concentration of $CuSO_4$ (0.23–0.28 M) and the time on the As recovery into the solution was studied. The process temperature has the greatest effect on the kinetics, while an increase in copper concentration from 0.23 to 0.28 M effects an increase in As transfer into solution from 93.2% to 97.8% for 120 min of leaching. However, the shrinking core model that best fits the kinetic data suggests that the process occurs by the intra-diffusion mode with the average activation energy of 44.9 kJ/mol. Using the time-to-a-given-fraction kinetics analysis, it was determined that the leaching mechanism does not change during the reaction. The semi-empirical expression describing the reaction rate under the studied conditions can be written as follows: $1/3\ln(1 - X) + [(1 - X) - 1/3 - 1] = 4560000Cu^{3.61}e^{-44900/RT}$ t.

Keywords: arsenic; trisulfide; copper sulfate; kinetics; leaching; shrinking core model; time-to-a-given-fraction kinetics analysis

1. Introduction

The need to increase the production of copper and other non-ferrous metals compels the industry to engage various primary and man-made low-grade polymetallic materials such as copper–zinc, copper–lead–zinc, poor arsenic-containing copper concentrates, enrichment products, etc. [1]. The overall decrease in the quality of mineral raw materials, combined with the use of arsenic-containing ores, results in large amounts of various intermediate products containing this highly toxic element [2].

Currently, copper concentrates and other copper-containing sulfide intermediates are most often processed by pyrometallurgical methods, while most impurities such as arsenic, lead, zinc, antimony are sublimated and passed to fine dusts during gas cleaning [3–10]. When such arsenic-containing materials are processed along with ore raw materials, arsenic is redistributed and accumulated in target products (matte, crude metal, etc.) [11] as well as intermediates (dust, sublimates, etc.) [12].

The currently used methods of separate processing of arsenic-containing materials only allow concentrating arsenic in separate products, but fail to address the environmental safety of the generated

waste containing active arsenic [13–15], and fail to produce effluent solutions with the concentration recommended by the World Health Organization (WHO) and the United States Environmental Protection Agency (USEPA) [16,17].

The use of hydrometallurgical technologies for these materials is complicated by the formation of multicomponent solutions and the difficulty of separating copper from arsenic [18–21].

Precipitation is a widely used method of removing arsenic from solutions [6,13,22–25]. The lowest soluble As compounds are arsenic sulfides [26], calcium arsenite, calcium arsenate [27,28] and iron arsenate [29–33]. Each of these precipitates exhibits relatively low solubility in the corresponding pH range, but these methods lead to loss of copper with arsenic-containing precipitates due to Cu co-precipitation, and do not yield high-quality respective copper products [20,29,34].

Arsenic precipitation as sulfide has the advantage of a high degree of Cu and As separation and water extraction due to the high specific gravity of As_2S_3. However, the residues are amorphous and heavily filtered. As_2S_3 is stable under acidic and reducing conditions (pH < 4), but is susceptible to atmospheric and bacterial oxidation. The solubility of arsenic sulfide is 1 mg/dm^3 at pH < 4.

In the works of Ke et al., and Lundström et al. [35,36] a method was proposed for the selective leaching of As from copper–arsenic intermediates in the presence of Cu(II) ions, based on their exchange reaction with As ions. This reaction was first described for the Nikkelverk process [35,37], which aimed at the separation of copper and nickel ions. Later it was described in the work of Lundström et al. [36].

In Japan, the application of this method is patented by Sumitomo [38,39]. The method allows efficient extraction of arsenic into the solution and its subsequent precipitation in the form of a well-filtered high-purity arsenic oxide. The solid residue of the leaching, consisting mainly of copper sulfide, can be further used in smelting.

According to the patent [40], arsenic cake is leached with an acidic solution with the addition of copper chloride. As a result, arsenic passes into solution, and copper precipitates as sulfide.

The work [21] describes the study to determine a method for processing mining and metallurgical acid effluents containing As and Cu. The proposed two-stage scheme includes precipitation of solutions containing up to 15% arsenic and up to 80% copper as sulfides by treating the solutions with hydrogen sulfide as a first stage, and selective leaching of arsenic from the obtained residue with the initial solution (which involves sulfide copper precipitation) as a second stage.

The mentioned works demonstrate the interest in this method from many researchers, since the need exists to process various arsenic-containing materials such as copper–arsenic, iron–arsenic gold-containing concentrates, dusts and various intermediates of copper and lead production, and many others. Loss of copper with arsenic waste and arsenic poisoning of target products are inevitable at various stages of processing such raw materials.

In our studies of hydrochemical processing of such materials [41,42], difficulties arise when separating copper and arsenic from the leachates. Therefore, in this study, we considered the physico-chemical aspects and mechanisms of the reactions during the leaching of arsenic trisulfide-based raw materials with water solutions of copper sulfate.

2. Materials and Methods

2.1. Materials and Reagents

The chemicals used in this study were of analytical grade; the water was distilled using a GFL-manufactured device (GFL mbH, Burgwedel, Germany). $CuSO_4 \cdot 5H_2O$ was obtained from AO Vekton (S-Petersburg, Russia).

The As_2S_3 containing material was obtained from an As-containing solution by reacting it with sodium hydrosulfide according to the method described elsewhere [43]. The chemical compositions of arsenic trisulfide-based raw material on a dry weight are presented in Table 1. The moisture content of the raw material was 60.2%.

Table 1. Chemical composition of arsenic trisulfide-based raw material, wt%.

Cu	As	S	Zn	Fe	Pb
0.14	40.20	44.86	0.42	0.23	1.24

2.2. Analysis

The chemical analysis of the original material and the resulting solid products of the studied processes was performed using an Axios MAX X-ray fluorescence spectrometer (XRF) (Malvern Panalytical Ltd., Almelo, The Netherlands). The chemical analysis of the obtained solutions was performed by mass spectrometry with inductively coupled plasma (ICP-MS) using an Elan 9000 instrument (PerkinElmer Inc., Waltham, MA, USA). The phase analysis was performed on an XRD 7000 Maxima diffractometer (Shimadzu Corp., Tokyo, Japan).

Scanning electron microscopy (SEM) was performed using a JSM-6390LV microscope (JEOL Ltd., Tokyo, Japan) equipped with an energy-dispersive X-ray spectroscopy analysis (EDS) module INCA Energy 450 X-Max 80 (Oxford Instruments, High Wycombe, UK).

Samples from each experiment were taken at the selected time intervals and analyzed using inductively coupled plasma mass spectrometry (ICP-MS–NexION 300S quadrupole mass spectrometer, PerkinElmer Inc., Waltham, MA, USA).

2.3. Experiments

Laboratory experiments on $CuSO_4$ leaching were carried out using an apparatus consisting of a 1 dm^3 borosilicate glass round bottom reactor (Lenz Laborglas GmbH & Co. KG, Wertheim, Germany), with openings for reagent injection, as well as for temperature control and removal of water vapor through a water-cooled reflux condenser. The reactor was thermostated. The materials were stirred using an overhead mixer at 400 rpm, which ensured uniform density of the pulp. A portion of the raw material weighing 60 g was added to a prepared solution of $CuSO_4$ of a required concentration. At the end of the experiment, the leaching pulp was filtered in a Buchner funnel (ECROSKHIM Co., Ltd., St. Petersburg, Russia); the solutions were sent for ICP-MS analysis; the leaching cake was washed with distilled water, dried at 100 °C to constant weight, weighed and sent for XRF analysis. All the experiments were performed twice and the mean values are presented here.

Eh-pH diagrams of the Cu-As-S-H_2O system were drawn using the HSC Chemistry Software Version 6.0 (Outokumpu Research Oy, Finland).

3. Results and Discussion

3.1. Thermodynamics of Leaching Arsenic Trisulfide with Copper-Containing Solution

Earlier, the thermodynamic features of the Cu-As-S-H_2O system were studied by Ke et al. [35], demonstrating that the temperature has practically no effect on the phase composition. So, Figure 1 shows the Pourbaix diagram of the Cu-As-S-H_2O system only at 80 °C. The concentration of Cu and As ions was 0.5 mol/dm^3, the concentration of S ions was 1 mol/dm^3. The diagram shows that the zone of existence of copper sulfide is in the pH range of 0 to 13 with Eh values of −0.7 to 0.4 V. So, under acidic conditions and with typical oxidation potentials, copper in the presence of S^{2-} or elemental S will be mainly in the form of copper sulfide. And according to [35] such conditions are actually created when arsenic-containing cakes are leached by copper cations. Arsenic trisulfide can also serve as a sulfur source. Under these conditions, it will either transform into arsenic trioxide or transfer to the solution as AsO_3^{3-} or AsO_4^{3-}. When the solution is supersaturated in arsenic and the system Eh is sufficiently high, the latter precipitates as oxide.

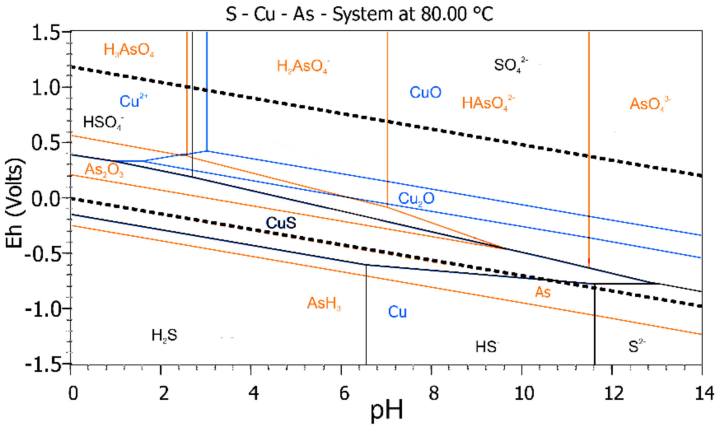

Figure 1. Pourbaix diagram of Cu-As-S-H_2O system at 80 °C: yellow—arsenic-containing phases; blue—copper-containing phases; black—sulfur-containing phases.

Figure 2 shows the X-ray diffraction patterns of the arsenic-containing raw materials and products obtained after leaching with different degrees of arsenic recovery: after 20 min of leaching at 80 °C (60% of As recovery) and after 240 min of leaching at 80 °C (more than 98% of As recovery). Liquid to solid ratio in both experiments was 10:1, copper concentration in initial solution—0.26 M.

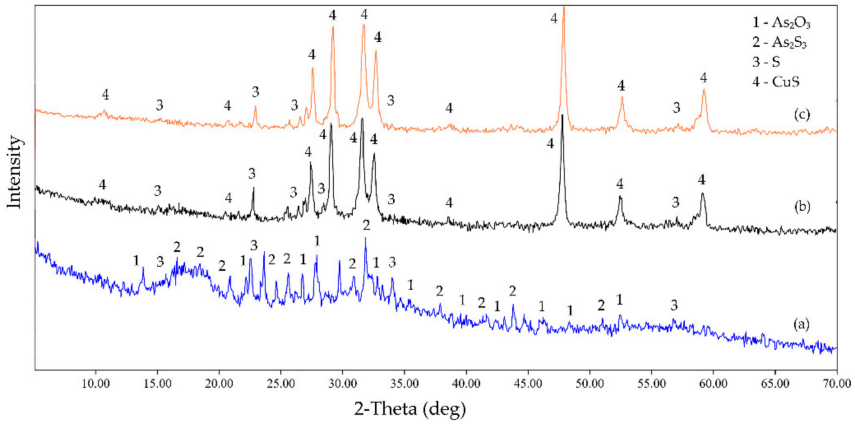

Figure 2. X-ray diffraction pattern of arsenic-containing raw material (**a**) and products of its leaching with copper sulfate at 60% recovery of As (**b**) and at more than 98% recovery of As (**c**).

Figure 2 shows that the arsenic-containing raw material contains amorphous material, as well as arsenic trisulfide and trioxide along with elemental S. While the leachates are mainly represented by copper sulfide and elemental S, higher degrees of the process completion result in smaller peaks for elemental sulfur, near complete reaction of the amorphous phase and a new crystalline phase, CuS.

Thus, the X-ray diffraction patterns confirm the previous [35] and our conclusions made regarding the thermodynamics of the process. Furthermore, the interaction of elemental S with copper cations is much slower than with arsenic trisulfide. A previous study assumed that the interaction of arsenic trisulfide with copper cations must proceed through the intermediate stages of elemental S and H_2S formation, since more negative Gibbs energies were obtained for these reactions [35]. Therefore, we also calculated the change in Gibbs free energy for the following chemical reactions (Equations (1)–(6)):

$$3CuSO_4(ia) + As_2S_3 + 6H_2O = 3CuS + 2H_3AsO_3(ia) + 3H_2SO_4(ia) \quad (1)$$

$$3CuSO_4(ia) + 4S + 4H_2O = 3CuS + 4H_2SO_4(ia) \quad (2)$$

$$CuSO_4(ia) + H_2S(ia) = CuS + H_2SO_4(ia) \quad (3)$$

$$As_2S_3 + H_2SO_4(ia) + 2H_2O = 2H_3AsO_3(a) + 4S \quad (4)$$

$$As_2S_3 + 3H_2O + 1.5O_2(g) = 2H_3AsO_3(a) + 3S \quad (5)$$

$$As_2S_3 + 6H_2O + 2O_2(g) = 2H_2S(ia) + 2H_3AsO_3(ia) + H_2SO_4(ia) \quad (6)$$

where ia—ionic./aqueous phase, g—gaseous phase.

The calculation results are presented in Figure 3, which shows the effect of temperature on the change in Gibbs free energy for each of the listed reactions.

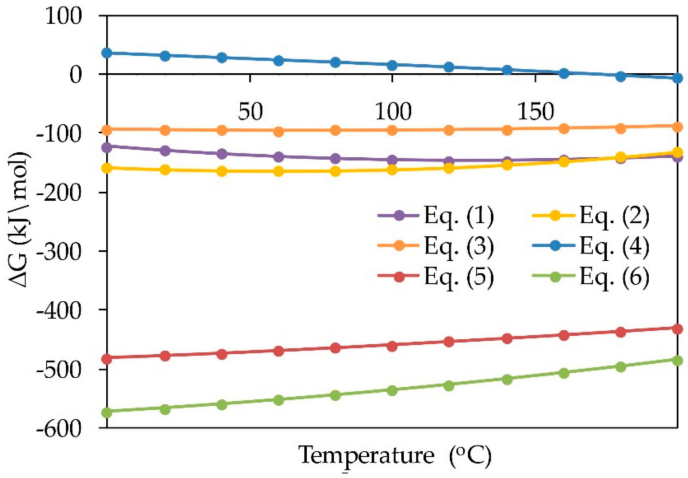

Figure 3. The calculation of the change in Gibbs free energy for Equations (1)–(6).

The calculations of the change in Gibbs free energy allow us to conclude that the probabilities of copper sulfate reaction with arsenic trisulfide, S, or H_2S (Equations (1)–(3)) are almost equal, although the change in Gibbs energy is lower in the presence of oxygen for the oxidation of arsenic trisulfide with the formation of elemental S and H_2S (Equations (5) and (6)). However, elemental S is still found in the cake, while arsenic almost completely passes into the solution (Figure 2). Therefore, it is likely that reaction 2 has a lower kinetic than reaction 1.

To determine if the reaction with elemental sulfur was kinetically controlled, we performed experiments on the effect of temperature on the Cu:S molar ratio of the product. The results of the experiments are presented in Figure 4. Notably, the degree of As extraction at all temperatures exceeded 95%, which means that the lower the Cu:S molar ratio in the leachate, the lower the reaction degree of the elemental sulfur.

Obviously, the Cu:S molar ratio of the leaching product approaches 1 as the temperature increases, which is consistent with the complete conversion of S into copper sulfide via reaction 2. Therefore, to accelerate this reaction, leaching under pressure at a temperature above 120 °C is necessary. In addition, reaction 2 slows down significantly at temperatures below 80 °C. The obtained data suggest that some of the As_2S_3 may generate elemental sulfur via reaction (5) and the reaction (2) of freshly formed sulfur also could have some kinetic difficulties.

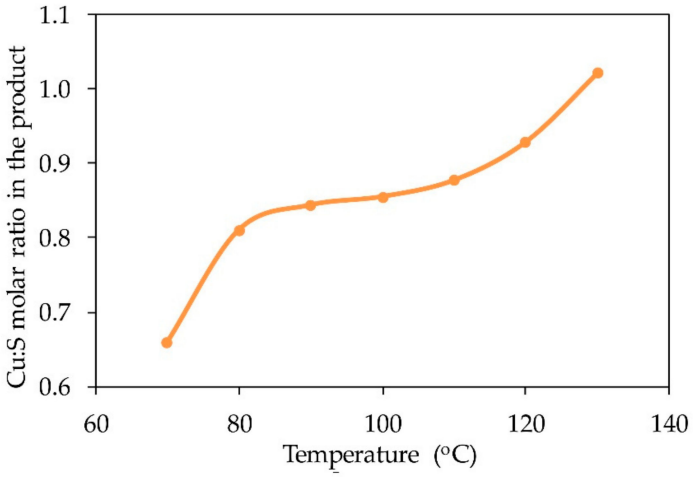

Figure 4. The effect of temperature on the Cu:S molar ratio in the leachate after 2 h of leaching with a 2-fold excess of copper in solution from the stoichiometry.

3.2. Effect of Process Parameters on As Recovery from Trisulfide

3.2.1. Effect of Temperature

As shown earlier, the initial material is highly amorphous and consists mainly of arsenic trisulfide. The effect of temperature and copper concentration on the leaching process was evaluated by As recovery in the solution. Figure 5 shows the dependence of As recovery on the duration and temperature. Liquid to solid ratio in all experiments was 10:1, copper concentration in initial solution—0.26 M.

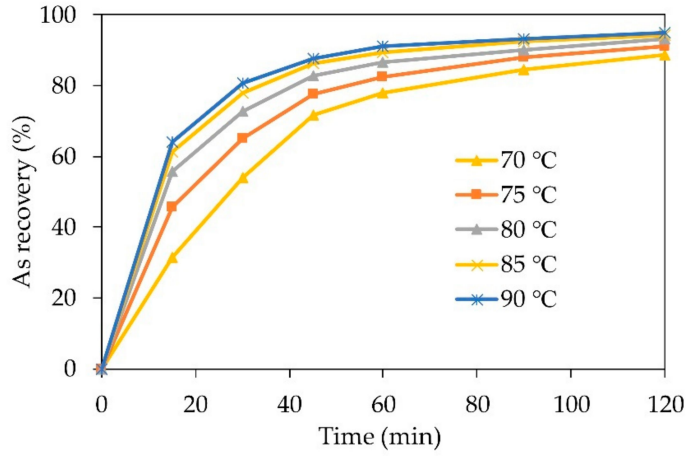

Figure 5. Dependence of the degree of As recovery from arsenic trisulfide on temperature and time.

Figure 5 shows a significant effect of temperature on the As recovery in the solution at the starting point of the process, from 0 to 60 min. At 90 °C, up to 80.7% of arsenic trisulfide is leached within 30 min. A decrease in temperature to 70 °C leads to a decrease in the degree of arsenic recovery to solution to 54.0% in a similar time.

An increase in the duration of leaching from 60 to 120 min leads to a decreased effect of temperature on the leaching of arsenic. Up to 88.6% of arsenic dissolves at 70 °C, and 94.9% at 90 °C within 120 min of the process. The data show that the temperature is the major factor in As recovery from arsenic trisulfide, which indicates kinetic control. However, a study of the kinetics is required to determine the limiting step.

3.2.2. Effect of Copper Concentration

The effect of copper concentration was evaluated in the concentration range 0.23–0.28 M, which corresponds to 90–110% of its stoichiometric requirement according to Equation (1). Liquid to solid ratio in all experiments was 10:1, temperature −80 °C.

The results in Figure 6 show the positive effect of copper concentration and leaching temperature on the dissolution of arsenic. An increase in copper concentration from 0.23 to 0.28 M effects an increase in As transfer into solution from 75.8% to 84.7% for 30 min of leaching, and from 93.2% to 97.8% for 120 min. Increasing the leaching time from 30 to 120 min leads to a decrease in the effect of copper concentration on the transition of arsenic to solution. A similar result was observed when studying the effect of temperature. The results also indicate that the influence of copper concentration has a lower value than temperature. However, the interval of concentration change was quite low.

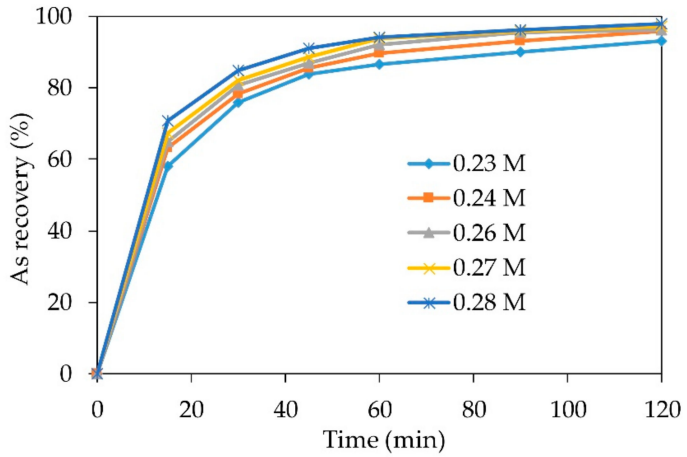

Figure 6. Dependence of As recovery on the concentration of copper in solution.

3.3. Characteristics of Residue

The cakes after leaching of arsenic trisulfide with a solution of copper sulfate were analyzed by scanning electron microscopy to assess the changes in the morphology of the sample. SEM images of the initial material and the cake after 240 min of leaching at 80 °C (more than 98% of As recovery) are presented in Figure 7.

According to the SEM images, the initial material is represented by 5–20 μm porous agglomerates of different shapes, with rough surfaces (Figure 7b). The apparent low level of crystallinity in this material is consistent with the X-ray phase analysis data shown in Figure 2. The interaction of arsenic sulfide with the copper ions in the solution forms agglomerates with lamellar, needle-like particles, the size of which are in the range 2–20 μm (Figure 7d,f).

SEM images of the surface of the formed particles with a magnification of 10,000 show the formation of 1–1.7 μm long and 100–130 nm thick plates on the surface of agglomerates (Figure 8).

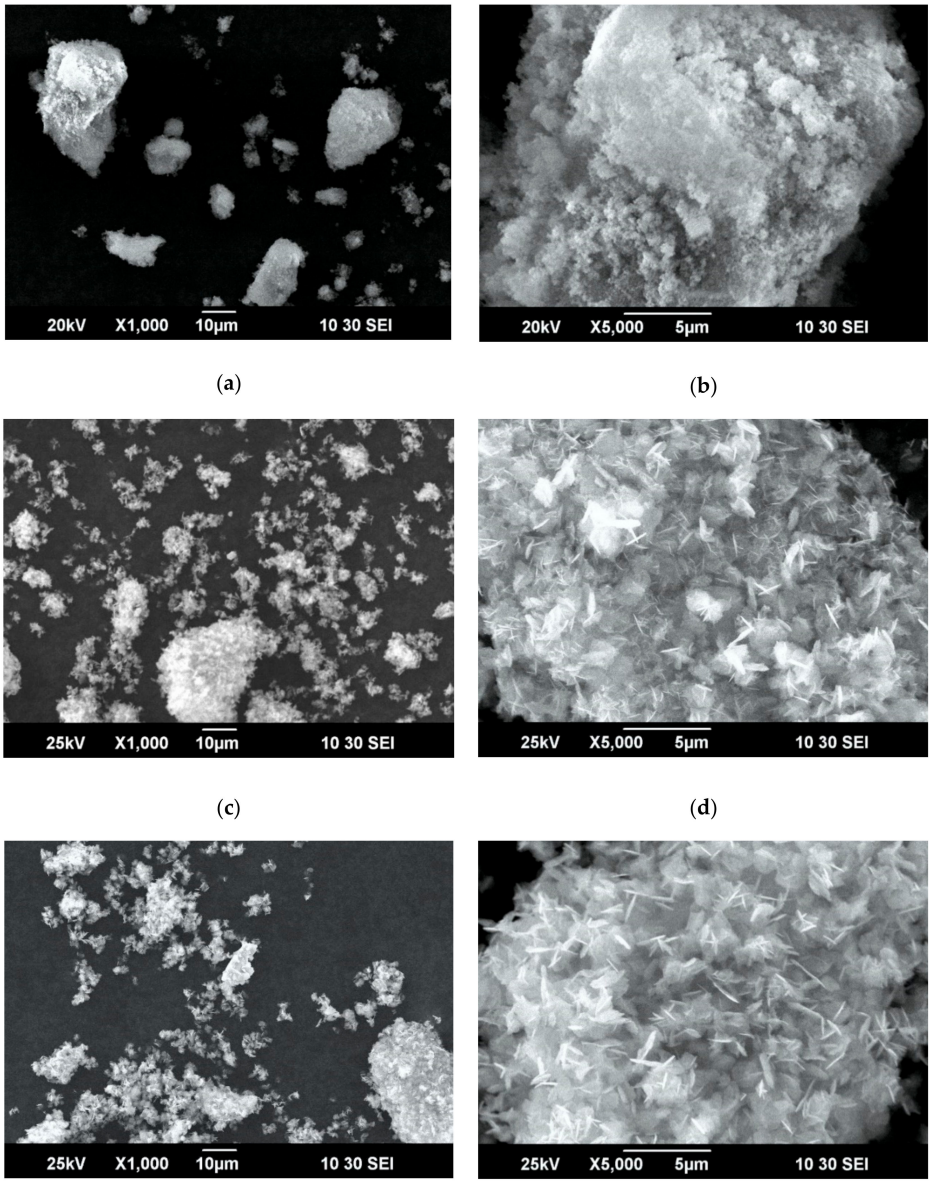

(**a**) (**b**)

(**c**) (**d**)

(**e**) (**f**)

Figure 7. Scanning electron microscopy (SEM) images of the initial material (**a**,**b**), filter cake after leaching of 60% arsenic (**c**,**d**), filter cake after complete extraction (**e**,**f**).

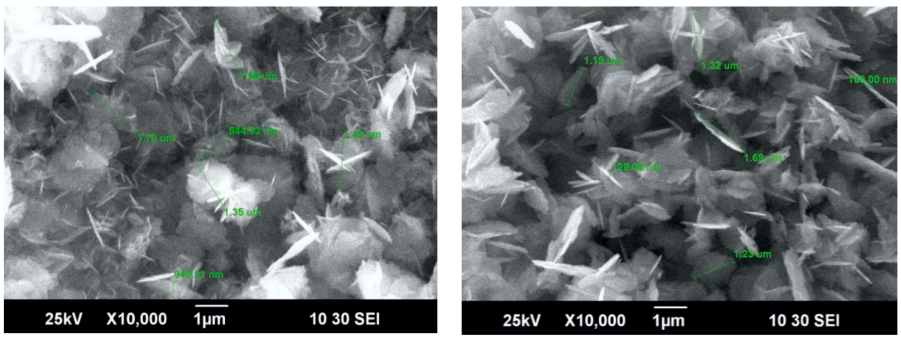

(**a**) (**b**)

Figure 8. SEM images of filter cake after leaching of 60% of arsenic (**a**) and filter cake after complete loosening (**b**).

The images show that the surface of the cake particles after 60% As recovery and after complete extraction are similar, but the plates are thicker after the leaching is complete (Figure 8a,b). Figure 9 shows energy dispersive spectroscopy microphotographs with points at which compositions were determined for the initial material and for cakes with varying degrees of As recovery (Table 2).

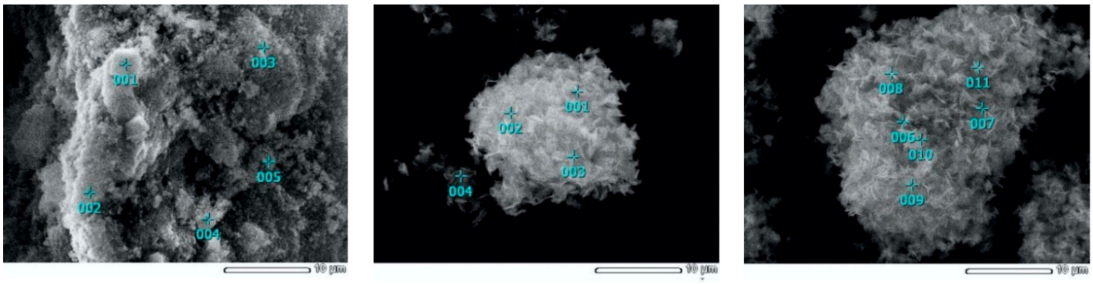

(**a**) (**b**) (**c**)

Figure 9. SEM images with points for determining by energy-dispersive X-ray spectroscopy analysis (EDS) the composition of the initial material (**a**), after 60% As recovery (**b**), full recovery (**c**).

Sulfur and arsenic are distributed unevenly, which is due to the presence of elemental sulfur in the initial material.

Arsenic trisulfide interacts with copper ions in the solution to form copper sulfide CuS, which is confirmed by the results of EDS and X-ray phase analysis (Figures 2 and 10). The copper content is 49–56% at 60% recovery of As, and increases to 57–64% when As is fully recovered.

Table 2. The results of energy dispersive spectroscopy, weight %.

Element	S	Fe	Cu	Zn	As	Total
Figure 9a. Point 001	52.8	0.4	2.8	2.8	41.2	100.0
Figure 9a. Point 002	39.6	0.4	4.7	3.9	51.4	100.0
Figure 9a. Point 003	61.4	0.3	2.9	2.6	32.7	100.0
Figure 9a. Point 004	51.2	0.2	3.1	3.2	42.3	100.0
Figure 9a. Point 005	64.6	0.3	2.7	2.2	30.2	100.0
Figure 9b. Point 001	44.4	0.1	51.4	0.5	3.6	100.0
Figure 9b. Point 002	40.7	0.2	56.0	0.4	2.7	100.0
Figure 9b. Point 003	45.2	0.1	48.5	1.1	5.1	100.0
Figure 9b. Point 004	39.4	0.0	54.3	1.0	5.3	100.0
Figure 9c. Point 006	39.8	0.0	60.2	0.0	0.0	100.0
Figure 9c. Point 007	41.6	0.1	57.4	0.3	0.6	100.0
Figure 9c. Point 008	41.1	0.0	58.2	0.3	0.4	100.0
Figure 9c. Point 009	35.6	0.0	64.4	0.0	0.0	100.0
Figure 9c. Point 010	41.5	0.1	58.0	0.2	0.1	100.0
Figure 9c. Point 011	42.7	0.1	56.9	0.0	0.3	100.0

Figure 10 shows that the copper content on the surface of the particles increases in the course of leaching. In the initial material (Figure 10b), copper is practically absent, only minor inclusions are found, as the copper was present in the solution from which the As_2S_3 containing raw material was precipitated. In the process of As recovery, the amount of copper sulfide on the surface increases (Figure 10b,e,h).

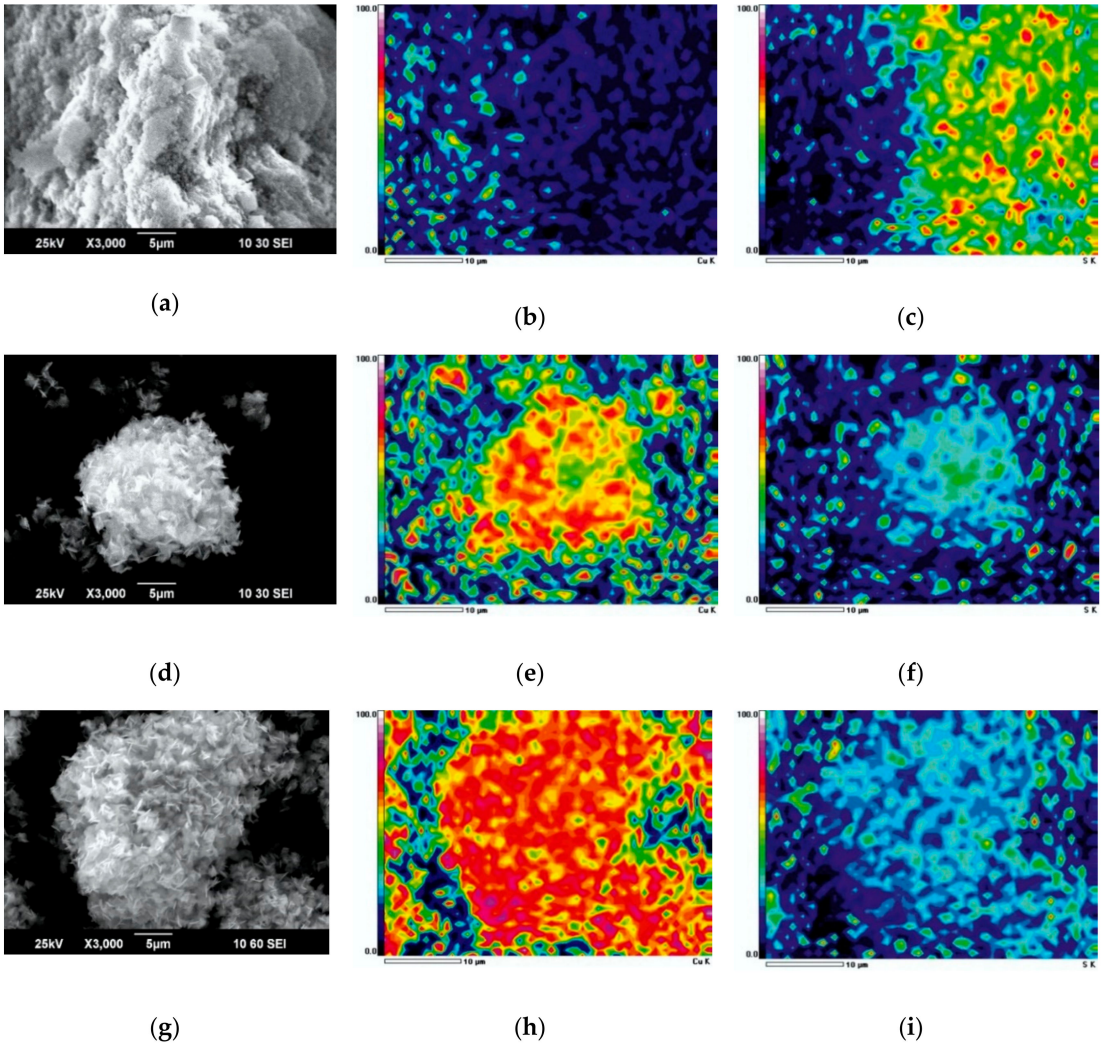

Figure 10. Microphotographs of the initial trisulfide (**a**), filter cake after leaching of 60% arsenic (**d**), filter cake after full recovery (**g**) and EDS mapping for copper (**b**,**e**,**h**) and sulfur (**c**,**f**,**i**).

Two theories exist to explain the mechanism of interaction of sulfides with copper ions [44]:

1. Interaction occurs immediately on the surface of the raw material, between the solid sulfur–sulfides and copper ions in the solution.
2. The process involves an intermediate stage of H_2S production when sulfides contact with acidified solutions. The H_2S then interacts with copper ions to form covellite.

SEM images, EDS, and EDS mapping suggest that in the process of arsenic extraction, the plates formed on the surface thicken, with a parallel increase in the copper content. The presence of plates or needle-shaped crystals on the surface (the predominant growth of crystals in one direction) and their thickening indicates that sulfide ions are being transported to the surface of existing particles and precipitation is initiated on the existing surfaces. So, arsenic trisulfide also could react with copper ions via the second mechanism.

3.4. Kinetic Model

The shrinking core model (SCM) is used to describe the kinetics of heterogeneous reactions, and suggests interaction of a substance with an external reagent only on the surface of the particles. The reaction zone gradually progresses inside the particles, leaving behind a converted product—an inert part of the particle. The core of the particle, containing the active component that has not

yet reacted, gradually decreases during the reaction. The change in unreacted core size is assumed to be linear, the kinetics of the process is also considered linear. This model assumes that the rate of the process is limited either by diffusion of the agent to the surface through the diffusion layer, diffusion through the product layer (film diffusion through the surface layer of the shrinking sphere), or chemical reaction for particles of constant or decreasing size. Thus, the shrinking core model not only describes how the process proceeds, as it can determine the basic kinetic characteristics, but explains the mechanism of the process as well.

The slowest stage with the highest resistance will be the rate limiting one, and its intensification will effect an increase the leaching efficiency.

Levenspiel [45] proposes several variants of the SCM. Our previous studies [46] showed that a new variant of SCM proposed by Dickenson and Heal [47] accurately describes the kinetics of leaching reactions regulated by interfacial transfer and diffusion through the product layer.

The correlation coefficients (R^2) obtained by modeling the leaching of arsenic trisulfide by copper sulfate solutions using the SCM equations are shown in Table 3.

Table 3. SCM equations fitting.

#	Limiting Step	Equation	R^2				
			70 °C	**75 °C**	**80 °C**	**85 °C**	**90 °C**
1	Diffusion through the product layer (sp)	$1 - 3(1 - X)^{2/3} + 2(1 - X)$	0.955	0.937	0.873	0.810	0.774
2	Diffusion through the product layer (pp)	X^2	0.899	0.815	0.696	0.606	0.557
3	Diffusion through the product layer (cp)	$X + (1 - X)\ln(1 - X)$	0.948	0.905	0.823	0.749	0.708
4	Diffusion through the liquid film (sp)	X	0.691	0.539	0.414	0.341	0.305
5	Surface chemical reactions (cp)	$1 - (1 - X)^{1/2}$	0.828	0.727	0.625	0.558	0.523
6	Surface chemical reactions (sp)	$1 - (1 - X)^{1/3}$	0.869	0.789	0.699	0.639	0.607
7	New shrinking core model	$1/3\ln(1 - X) + [(1 - X)^{-1/3} - 1]$	0.968	0.985	0.993	0.991	0.987

Sp—spherical particles, pp—prismatic particles, cp—conus particles, X—the degree of As recovery into the solution.

According to the table data, the new SCM version (Equation (7) in Table 3) describes the derived dependences better than all other equations and has the highest correlation coefficients for the studied temperatures (R^2), which confirms that leaching proceeds in the intra-diffusion area.

To calculate the activation energy, we plotted the dependence of $\ln k_c$ vs. 1/T, where k_c is the slope of each straight line obtained by substituting the experimental data into the SCM Equation (7) in Table 3, as can be seen in Figure 11a. Based on Equation (7), derived from Arrhenius law, we used the slope of the line to determine the apparent activation energy 44.9 kJ/mol. As shown before [48], a high value of the activation energy is not always representative of a kinetically controlled reaction.

$$\ln k_c = \ln A - E_a/RT. \quad (7)$$

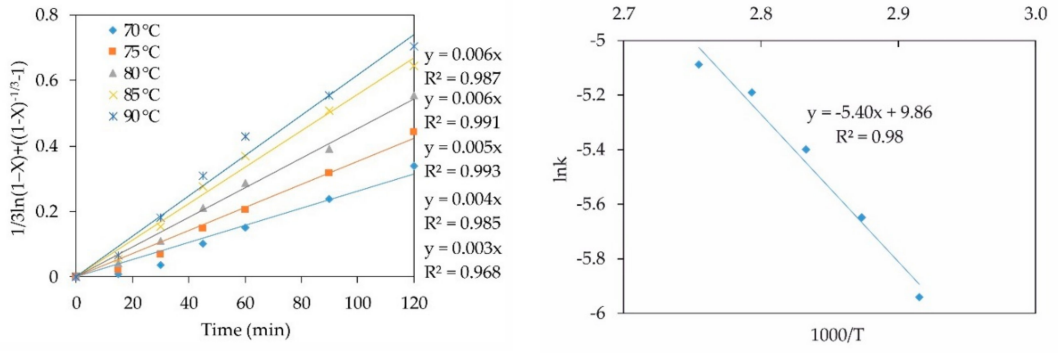

(**a**) (**b**)

Figure 11. Calculating angular coefficients k_c (**a**), reverse dependence of $\ln k_c$ on temperature (**b**).

The Eyring equation (Equations (8) and (9)) (transition state theory) was used to calculate other kinetic characteristics, including enthalpies and entropies [49,50].

$$k_c = \frac{k_b T}{h} e^{\Delta G^{++}/RT}. \quad (8)$$

$$T * \ln\frac{k_c}{T} = T * \left(\ln\frac{k_b}{h} + \frac{\Delta S^{++}}{R}\right) - \frac{\Delta H^{++}}{R} \quad (9)$$

where $k_b = 1.381 \times 10^{-23}$ J/K (Boltzmann constant) and $h = 6.626 \times 10^{-34}$ J·s (Planck constant).

The values ΔH^{++} and ΔS^{++} can be used to calculate the free energy as per Equation (10).

$$\Delta G^{++} = \Delta H^{++} - T\Delta S^{++}. \quad (10)$$

Activation enthalpy and entropy were calculated graphically by plotting the temperature dependence in the reference frame $T \cdot \ln(k_c/T)$ (Figure 12).

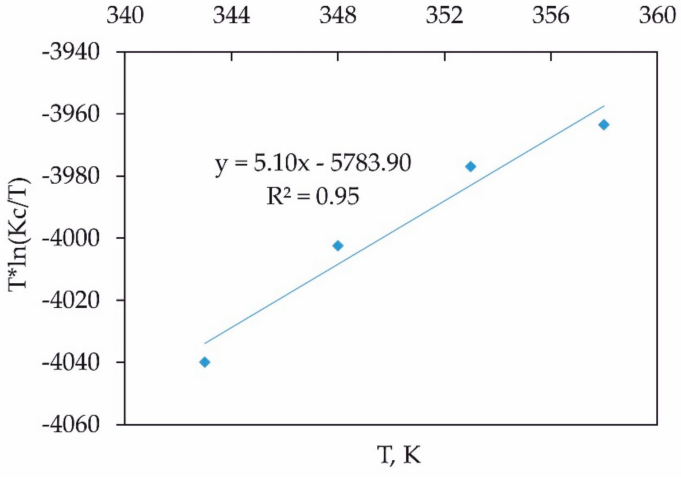

Figure 12. Eyring plot for arsenic leaching.

The enthalpy and activation entropy values obtained from the plot were 48.1 kJ/mol and −155.1 J/(mol·K). The small difference between the activation energies and the enthalpies is due to the low temperatures of the process (Equation (11)).

$$E_a = \Delta H^{++} + RT. \quad (11)$$

The negative values of entropy and positive values of free energy, enthalpy, indicate a non-spontaneous reaction in the entire range of temperatures studied.

Using the slope of the straight lines obtained by substituting the new SCM model with copper concentrations of 0.23–0.28 M and a temperature of 8 °C, a graph in the $\ln k_c$ vs. lnCu frame of reference was obtained to determine the reaction order with respect to Cu. The resulting empirical order with respect to Cu was 3.61 (Figure 13).

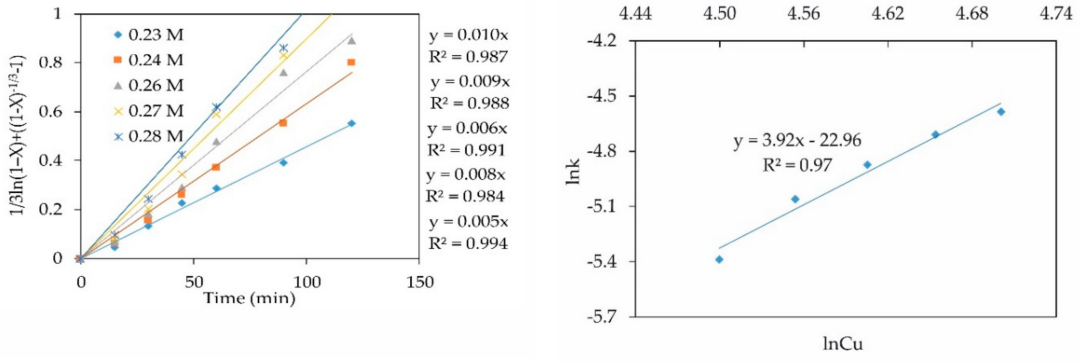

(**a**) (**b**)

Figure 13. Dependence of the new SCM equation on time (**a**), and $\ln k_c$ vs. lnCu for determining the order with respect to copper concentration (**b**).

By substituting the Arrhenius equation into the equation of the new shrinking core model, we can obtain Equation (12):

$$1/3\ln(1 - X) + [(1 - X)^{-1/3} - 1] = k_o e^{-E_a/RT} t. \quad (12)$$

In Equation (12), k_o depends on the initial concentration of copper in the solution; Equation (12) can be represented as follows (Equation (13)):

$$1/3\ln(1 - X) + [(1 - X)^{-1/3} - 1] = k_o Cu^n e^{-E_a/RT} t \quad (13)$$

where n is the order with respect to copper concentration.

Based on the earlier results, we can derive the following equation for leaching of arsenic trisulfide with copper sulfate solutions (Equation (14)):

$$1/3\ln(1 - X) + [(1 - X)^{-1/3} - 1] = k_o Cu^{3.61} e^{-44900/RT} t. \quad (14)$$

Graphs were plotted for all temperatures and copper concentrations, which allowed us to determine a fixed angle of inclination a = 4,560,000. The value of a obtained graphically and the corresponding value of the correlation coefficient R^2 are shown in Figure 14. The obtained value of coefficient "a" corresponds to k_o.

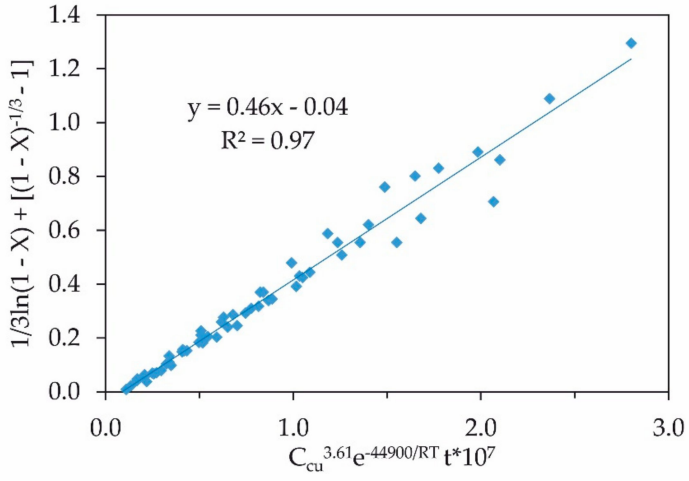

Figure 14. Graph for determining k_0.

Based on the data in Figure 14, k_o = 4,560,000, and therefore the kinetic Equation (15) is as follows:

$$1/3\ln(1 - X) + [(1 - X)^{-1/3} - 1] = 4560000Cu^{3.61}e^{-44900/RT}\ t. \quad (15)$$

Although an SCM is often used in hydrometallurgical kinetics to determine the activation energy of processes and to derive empirical equations, it has some drawbacks. For example, this method only allows us to determine the average values of the activation energy, which may lead to the omission of certain features of the reactions. It is therefore necessary to determine the kinetic characteristics during the process, which may change, e.g., due to the slower kinetics for the reaction of copper cations with elemental S. For this purpose, the time-to-a-given-fraction method [51] was used, allowing us to calculate the apparent activation energy at different points of the leaching process. The time required to achieve a certain degree of leaching and the apparent activation energy E_a are related as per Equation (16).

$$\ln t_x = \text{const} - \ln A + E_a/RT. \quad (16)$$

The slope of the graph plotted in the reference frame $\ln t_x$ vs. 1/T allowed us to calculate the apparent activation energy.

Figure 15 shows the graphical calculation of the apparent activation energy for different degrees of arsenic recovery.

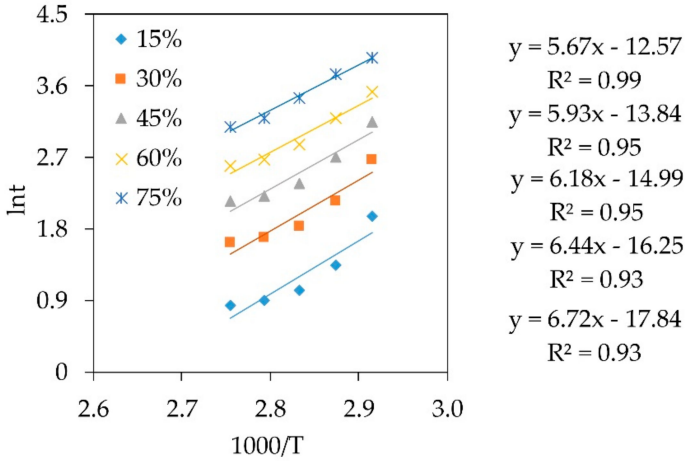

Figure 15. Dependence of $\ln t_x$ on 1/T for different degrees of As recovery in solution.

As seen in Figure 15, the values of the apparent activation energy calculated using the time-to-a-given-fraction method vary from 47.1 to 55.9 kJ/mol as the degree of arsenic recovery in solution increases from 15% to 75%. These values coincide with the previously obtained value of the SCM apparent activation energy, and confirm that the reaction mechanism does not change during leaching. However, a high activation energy at the later stage of leaching may be necessary for the reaction of elemental S (Figure 4), which may envelope arsenic sulfide and prevent more complete leaching of As.

4. Conclusions

This work studied the kinetics of the selective separation of copper and arsenic products by leaching arsenic trisulfide with a solution of copper sulfate. The study provides new data on the behavior of the initial components in the leaching process, using new approaches to studying the reaction kinetics. The conclusions are as follows:

1. The original arsenic sulfide material contains a substantial amorphous phase and, thermodynamically, an exchange reaction to form copper sulfide and various arsenic oxides should take place in the presence of copper sulfate in the entire studied temperature range. However, the leaching mechanisms may vary, since at the starting point arsenic sulfide is likely to be oxidized to form elemental sulfur or H_2S, which only then go on to react with copper cations.
2. Achieving the stoichiometric composition of copper sulfide in the final product is possible only with a large excess of copper cations and at increased temperature, which is due to the slow kinetics of the reaction of elemental sulfur with copper cations.
3. SEM images, EDS, and EDS mapping demonstrate that solid sulfur–sulfides react with copper ions. H_2S also could be generated and can react with the copper.
4. At 90 °C, up to 80.7% of arsenic trisulfide is leached within 30 min. A decrease in temperature to 70 °C leads to a decrease in the degree of arsenic recovery to solution to 54.0% in a similar time. Up to 88.6% of arsenic dissolves at 70 °C, and 94.9% at 90 °C within 120 min. This shows a significant effect of temperature on the As recovery. An increase in copper concentration from 0.23 to 0.28 M effects an increase in As transfer into solution from 75.8% to 84.7% for 30 min of leaching, and from 93.2 to 97.8% for 120 min.
5. The process temperature has the greatest effect on the kinetics. However, the shrinking core model that best fits the data suggests the process occurs by the intra-diffusion mode with the average activation energy of 44.9 kJ/mol.
6. Using the time-to-a-given-fraction kinetics analysis, it was determined that the leaching mechanism does not change during the reaction. The value of activation energy during the reaction increases from 47.1 kJ/mol at 15% arsenic recovery to 55.9 kJ/mol at 75%. This may be due to the slow kinetics of elemental sulfur reacting with copper cations.
7. Based on the findings, a semi-empirical equation was obtained, which allows us to describe the kinetics of the leaching of arsenic-containing cake by copper cations with a great accuracy: $1/3\ln(1 - X) + [(1 - X)^{-1/3} - 1] = 4560000Cu^{3.61}e^{-44900/RT}\ t$.

Author Contributions: Conceptualization, D.A.R.; methodology, K.A.K. and A.A.S.; validation, E.A.K..; formal analysis, K.A.K., D.A.R.; investigation, A.A.S. and E.A.K.; resources, E.A.K., D.A.R.; data curation, D.A.R.; writing—original draft preparation, K.A.K.; writing—review and editing, A.A.S., D.A.R.; visualization, A.A.S., K.A.K.; supervision, A.A.S.; project administration, D.A.R.; funding acquisition, D.A.R. All authors have read and agreed to the published version of the manuscript.

Funding: The research was funded by the Russian Science Foundation, grant number 18-19-00186. The SEM/EDS analyses were funded by State Assignment, grant number 10.7347.2017/8.9.

Acknowledgments: Technicians at Ural Branch of the Russian Academy of Sciences are acknowledged for their assistance with XRD, XRF, SEM, EDS, and ICP-MS analysis.

Conflicts of Interest: The authors declare no conflict of interest. The funders had no role in the design of the study; in the collection, analyses, or interpretation of data; in the writing of the manuscript, or in the decision to publish the results.

References

1. Celep, O.; Alp, İ.; Deveci, H. Improved gold and silver extraction from a refractory antimony ore by pretreatment with alkaline sulphide leach. *Hydrometallurgy* **2011**, *105*, 234–239. [CrossRef]
2. Bissen, M.; Frimmel, F.H. Arsenic–A review. Part I: Occurrence, Toxicity, Speciation, Mobility. *Acta Hydroch. Hydrob.* **2003**, *31*, 9–18. [CrossRef]
3. Shibayama, A.; Takasaki, Y.; William, T.; Yamatodani, A.; Higuchi, Y.; Sunagawa, S.; Ono, E. Treatment of smelting residue for arsenic removal and recovery of copper using pyro–hydrometallurgical process. *J. Hazard. Mater.* **2010**, *181*, 1016–1023. [CrossRef] [PubMed]
4. Long, G.; Peng, Y.; Bradshaw, D. A review of copper–arsenic mineral removal from copper concentrates. *Miner. Eng.* **2012**, *36–38*, 179–186. [CrossRef]
5. Dalewski, F. Removing Arsenic from Copper Smelter Gases. *JOM* **1999**, *51*, 24–26. [CrossRef]
6. Vircikova, E.; Havlik, M. Removing As from Converter Dust by a Hydrometallurgical Method. *JOM* **1999**, *51*, 20–23. [CrossRef]
7. Piret, N.L. The Removal and Safe Disposal of Arsenic in Copper Processing. *JOM* **1999**, *51*, 16–17. [CrossRef]
8. Cheng, R.; Ni, H.; Zhang, H.; Zhang, X.; Bai, S. Mechanism research on arsenic removal from arsenopyrite ore during a sintering process. *Int. J. Min. Met. Mater.* **2017**, *24*, 353–359. [CrossRef]
9. Safarzadeh, M.S.; Miller, J.D. Reaction of Enargite (Cu_3AsS_4) in Hot Concentrated Sulfuric Acid under an Inert Atmosphere. Part II: High-quality Enargite. *Int. J. Miner. Process.* **2014**, *128*, 79–85. [CrossRef]
10. Liu, J.; Chi, R.; Xu, Z.; Zeng, Z.; Liang, J. Selective arsenic-fixing roast of refractory gold concentrate. *Metall. Mater. Trans. B* **2000**, *31*, 1163–1168. [CrossRef]
11. Safarzadeh, M.S.; Miller, J.D. Reaction of Enargite (Cu_3AsS_4) in Hot Concentrated Sulfuric Acid under an Inert Atmosphere. Part I: Enargite Concentrate. *JOM* **2014**, *128*, 68–78. [CrossRef]
12. Ritcey, G.M. Tailings management in gold plants. *Hydrometallurgy* **2005**, *78*, 3–20. [CrossRef]
13. Riveros, P.A.; Dutrizac, J.E.; Spencer, P. Arsenic disposal practices in the metallurgical industry. *Can. Metall. Q.* **2001**, *40*, 395–420. [CrossRef]
14. Smedley, P.L.; Kinniburgh, D.G. A review of the source, behaviour and distribution of arsenic in natural waters. *Appl. Geochem.* **2002**, *17*, 517–568. [CrossRef]
15. Yao, L.; Min, X.; Xu, H.; Ke, Y.; Liang, Y.; Yang, K. Hydrothermal Treatment of Arsenic Sulfide Residues from Arsenic-Bearing Acid Waste Water. *J. Environ. Res. Public Health* **2018**, *15*, 1863. [CrossRef]
16. Smith, A.H.; Smith, M.M.H. Arsenic drinking water regulations in developing countries with extensive exposure. *Toxicology* **2004**, *198*, 39–44. [CrossRef]
17. Shoppert, A.; Loginova, I.; Rogozhnikov, D.; Karimov, K.; Chaikin, L. Increased As Adsorption on Maghemite-Containing Red Mud Prepared by the Alkali Fusion-Leaching Method. *Minerals* **2019**, *9*, 60. [CrossRef]
18. Nazari, A.M.; Radzinski, R.; Ghahreman, A. Review of arsenic metallurgy: Treatment of arsenical minerals and the immobilization of arsenic. *Hydrometallurgy* **2017**, *174*, 258–281. [CrossRef]
19. Ruiz, M.C.; Vera, M.V.; Padilla, R. Mechanism of enargite pressure leaching in the presence of pyrite. *Hydrometallurgy* **2011**, *105*, 290–295. [CrossRef]
20. Anderson, C.G.; Twidwell, L.G. Hydrometallurgical processing of gold-bearing copper enargite concentrates. *Can. Metall. Q.* **2008**, *47*, 337–346. [CrossRef]
21. Jiang, G.M.; Bing, P.E.N.G.; Chai, L.Y.; Wang, Q.W.; Shi, M.Q.; Wang, Y.Y.; Hui, L.I.U. Cascade sulfidation and separation of copper and arsenic from acidic wastewater via gas–liquid reaction. *Trans. Nonferrous Met. Soc. China* **2017**, *27*, 925–931. [CrossRef]
22. Jiang, J.Q. Research progress in the use of ferrate(VI) for the environmental remediation. *J. Hazard. Mater.* **2007**, *146*, 617–623. [CrossRef] [PubMed]
23. Prucek, R.; Tuček, J.; Kolařík, J.; Filip, J.; Marušák, Z.; Sharma, K.; Zbořil, R. Ferrate(VI)-induced arsenite and arsenate removal by in situ structural incorporation into magnetic iron(III) oxide nanoparticles. *Environ. Sci. Technol.* **2013**, *47*, 3283–3292. [CrossRef] [PubMed]

24. Lee, Y.; Um, I.H.; Yoon, J. Arsenic(III) oxidation by iron(VI) (ferrate) and subsequent removal of arsenic(V) by iron(III) coagulation. *Environ. Sci. Technol.* **2003**, *37*, 5750–5756. [CrossRef]
25. Gomez, M.A.; Becze, L.; Blyth, R.I.R.; Cutler, J.N.; Demopoulos, G.P. Molecular and structural investigation of yukonite (synthetic & natural) and its relation to arseniosiderite. *Geochim. Cosmochim. Acta* **2010**, *74*, 5835–5851. [CrossRef]
26. Guo, L.; Du, Y.; Yi, Q.; Li, D.; Cao, L.; Du, D. Efficient removal of arsenic from "dirty acid" wastewater by using a novel immersed multi-start distributor for sulphide feeding. *Sep. Purif. Technol.* **2015**, *142*, 209–214. [CrossRef]
27. Moon, D.H.; Dermatas, D.; Menounou, N. Arsenic immobilization by calcium–arsenic precipitates in lime treated soils. *Sci. Total Environ.* **2004**, *330*, 171–185. [CrossRef]
28. Zhu, Y.N.; Zhang, X.H.; Xie, Q.L.; Wang, D.Q.; Cheng, G.W. Solubility and stability of calcium arsenates at 25 °C. *Water Air Soil Pollut.* **2006**, *169*, 221–238. [CrossRef]
29. Gomez, M.A. The effect of copper on the precipitation of scorodite ($FeAsO_4{\cdot}2H_2O$) under hydrothermal conditions: Evidence for a hydrated copper containing ferric arsenate sulfate-short lived intermediate Original Research Article. *J. Colloid Interface Sci.* **2011**, *360*, 508–518. [CrossRef]
30. Fujita, T.; Taguchi, R.; Abumiya, M.; Matsumoto, M.; Shibata, E.; Nakamura, T. Effects of zinc, copper and sodium ions on ferric arsenate precipitation in a novel atmospheric scorodite process. *Hydrometallurgy* **2008**, *93*, 30–38. [CrossRef]
31. Yang, B.; Zhang, G.L.; Deng, W.; Ma, J. Review of arsenic pollution and treatment progress in nonferrous metallurgy industry. *Adv. Mater. Res.* **2013**, *634–638*, 3239–3243. [CrossRef]
32. Caetano, M.L.; Ciminelli, S.; Rocha, S.D.; Spitale, M.C.; Caldeira, C.L. Batch and continuous precipitation of scorodite from dilute industrial solutions. *Hydrometallurgy* **2009**, *95*, 44–52. [CrossRef]
33. Monhemius, A.J.; Swash, P.M. Removing and stabilizing as from copper refining circuits by hydrothermal processing. *JOM* **1999**, *51*, 30–33. [CrossRef]
34. Morales, A.; Cruells, M.; Roca, A.; Bergó, R. Treatment of copper flash smelter flue dusts for copper and zinc extraction and arsenic stabilization. *Hydrometallurgy* **2010**, *105*, 148–154. [CrossRef]
35. Ke, Y.; Shen, C.; Min, X.B.; Shi, M.Q.; Chai, L.Y. Separation of Cu and As in Cu-As-containing filter cakes by Cu^{2+}-assisted acid leaching. *Hydrometallurgy* **2017**, *172*, 45–50. [CrossRef]
36. Lundström, M.; Liipo, J.; Taskinen, P.; Aromaa, J. Copper precipitation during leaching of various copper sulfide concentrates with cupric chloride in acidic solutions. *Hydrometallurgy* **2016**, *166*, 136–142. [CrossRef]
37. Crundwell, F.K.; Moats, M.; Ramachandran, V. *Hydrometallurgical Production of High-Purity Nickel and Cobalt, Extractive Metallurgy of Nickel, Cobalt and Platinum Group Metals*; Elsevier: Oxford, UK, 2011; pp. 281–299. [CrossRef]
38. Toshimasa, I.; Yoshio, M. Method for Separating and Recovering Arsenious Acid from Substance Containing Arsenic Sulfide. J.P. Patent S59107923, 22 June 1984.
39. Tadashi, N.; Yoshio, M.; Naoki, K. Recovery of Arsenious Acid from Substance Containing Arsenic Sulfide. J.P. Patent S5869723, 26 April 1983.
40. Gong, D.; Gong, H.; Li, C.H. Method for Recovering Simple Substance Arsenic from Arsenic Sulfide Slag. C.N. Patent 101386915, 18 March 2009.
41. Karimov, K.A.; Naboichenko, S.S. Sulfuric Acid Leaching of High-Arsenic Dust from Copper Smelting. *Metallurgist* **2016**, *60*, 456–459. [CrossRef]
42. Karimov, K.A.; Naboichenko, S.S.; Kritskii, A.V.; Tret'yak, M.A.; Kovyazin, A.A. Oxidation Sulfuric Acid Autoclave Leaching of Copper Smelting Production Fine Dust. *Metallurgist* **2019**, *62*, 1244–1249. [CrossRef]
43. Mamyachenkov, S.V.; Anisimova, O.S.; Kostina, D.A. Improving the precipitation of arsenic trisulfide from washing waters of sulfuric-acid production of copper smelteries. *Russ. J. Non Ferr. Met.* **2017**, *58*, 212–217. [CrossRef]
44. Nabojčenko, S.S. (Ed.) *Avtoklavnaja Gidrometallurgija Cvetnych Metallov*; GOU UGTU-UPI: Ekaterinburg, Russia, 2002; ISBN 978-5-321-00065-6. (In Russia)
45. Levenspiel, O. *Chemical Reaction Engineering*, 3rd ed.; Wiley: New York, NY, USA, 1999; ISBN 978-0-471-25424-9.
46. Rogozhnikov, D.A.; Shoppert, A.A.; Dizer, O.A.; Karimov, K.A.; Rusalev, R.E. Leaching Kinetics of Sulfides from Refractory Gold Concentrates by Nitric Acid. *Metals* **2019**, *9*, 465. [CrossRef]

47. Dickinson, C.F.; Heal, G.R. Solid-liquid diffusion controlled rate equations. *Thermochim. Acta* **1999**, *340*, 89. [CrossRef]
48. Gok, O.; Anderson, C.G.; Cicekli, G.; Cocen, E.I. Leaching kinetics of copper from chalcopyrite concentrate in nitrous-sulfuric acid. *Physicochem. Probl. Mi.* **2014**, *50*, 399–413. [CrossRef]
49. Hidalgo, T.; Kuhar, L.; Beinlich, A.; Putnis, A. Kinetic study of chalcopyrite dissolution with iron(III) chloride in methanesulfonic acid. *Miner. Eng.* **2018**, *125*, 66–74. [CrossRef]
50. Lente, G.; Fábián, I.; Poë, A.J. A common misconception about the Eyring equation. *New J. Chem.* **2005**, *29*, 759. [CrossRef]
51. Hidalgo, T.; Kuhar, L.; Beinlich, A.; Putnis, A. Kinetics and mineralogical analysis of copper dissolution from a bornite/chalcopyrite composite sample in ferric-chloride and methanesulfonic-acid solutions. *Hydrometallurgy* **2019**, *188*, 140–156. [CrossRef]